INCLUSIVE PUBLISHING
TRUSTED SCIENCE

PAPER • OPEN ACCESS

A thin transferable blue light-emitting diode by electrochemical lift-off

View the article online for updates and enhancements.

NANO EXPRESS

A thin transferable blue light-emitting diode by electrochemical lift-off

Yaonan Hou[1,4,5] ⬤, Yong Wang[2] and Qingkang Ai[3]

1   School of Microelectronics, Shandong University, No. 1500 Shunhua Road, Lixia District, Jinan, Shandong Province, 250101, People's Republic of China
2   School of Information and Communication Engineering, University of Electronic Science and Technology of China, No.2006, Xiyuan Ave, West Hi-Tech Zone, Chengdu, Sichuan, Chengdu, 611731, People's Republic of China
3   Beijing Laize Photonics, Co. Ltd, No.1 Shunqiang Road, Shunyi District, Beijing, 101339, People's Republic of China
4   The author's current address: Optoelectronics Research Centre, University of Southampton, University Road, Southampton, SO17 1BJ United Kingdom.
5   Author to whom any correspondence should be addressed.

E-mail: houyaonan@gmail.com and yongwang@uestc.edu.cn

Abstract

We demonstrate a transferable blue light-emitting diode (LED) fabricated using a cost-effective approach. By means of solution-based electrochemical etching, an ultrathin free-standing membrane can be obtained from a commercial III-nitride LED wafer. The membrane, containing a full LED structure (including p-/n-type layers and multiple quantum wells) epitaxially grown on a sapphire substrate, is transferable to foreign substrates with a simple lift-off process facilitated by electrochemical etching. After fabrication, optical properties of the thin film are massively improved, accompanied by a 17-fold enhanced photoluminescence normal to the film surface. Prototype transferable blue LEDs are realized on both a copper-coated glass substrate and a polypropylene substrate. The devices exhibit a high performance with bright emission at 447 nm under electrical injection at room temperature.

1. Introduction

Flexible light-emitting diodes (LEDs) have attracted much attentions because of their promising applications in foldable-displays [1], smart-clothing [2], biomedical analysis [3], and visible-light communications [4]. Organic LEDs (OLEDs) and colloidal quantum dot LEDs (CQD-LEDs) have been developed and studied in the last two decades for this purpose [5, 6]. Compared with such devices, III-nitride semiconductor LEDs have a higher internal quantum efficiency (IQE), a better chemical stability and a longer lifespan, especially a broader waveband extending to the blue-ultraviolet (UV) region [7, 8]. However, high-brightness III-nitride LEDs require a low-defect density, which is only achievable on special rigid substrates (e. g. sapphire and Si) by epitaxially growth [9], despite that some groups demonstrated transferable III-nitride films grown on two-dimensional materials [10–12]. In addition, owing to the large refractive index (2.4), the critical angle of III-nitrides is as small as ~23°, which leads to a small light extraction efficiency (LEE). Therefore, it is imperative to develop a technique to transfer the high-brightness III-nitride films from their host substrates to foreign ones, while enhancing (at least not deteriorating) the IQE and LEE.

Conventional methods to release the III-nitride epitaxial layers utilize laser lift-off or chemical etching [3, 13–16]. The former approach requires high-power UV laser, which is employed to melt the GaN layer close to the substrate side by back illumination. This technique has been demonstrated useful in transferring high-quality LEDs to an arbitrary substrate [17–19], but the involvement of expensive lasers, double-side polished transparent substrates and low yields increases the cost [20]. In 2011, Kim *et al* developed a method to transfer III-nitride LEDs by chemical etching the Si (111) substrate using KOH solution [21]. The anisotropic etching introduces thin anchor bars underneath the epitaxial film, facilitating the transfer process. This method has a

high throughput in generating large-area transferable micro-LEDs. However, the alkaline solution is also corrosive to III-nitrides [22, 23]. Recent work reveals that electrochemical etching away the host substrate is a prospective way to fabricate transferable III-nitride devices [24–33]. Compared with chemical etching, electrochemical etching provided a higher flexibility to enhance the controllability (thus the selectivity) via adjusting the external bias (e.g. value, time, direction and so on) [34–36]. Apart from chemical etching, photoelectrochemical etching has been developed to transfer III-nitride films [37–41]. Such a process needs to be carried out with the assistance of light illumination from the backside to remove a sacrificial layer. It is found that pyramid-like nano-cones can form by etching c-plane GaN, which is helpful to improve LEE [41]. In comparison, electrochemical etching is reported to introduce either nanopores or complete etching (polishing) depending on the conditions [42]. However, there is limited work in electrochemical lift-off technology, obtaining high quality free-standing (FS) films for transferable LEDs is still extremely challenging [27, 43]. In this work, we present an approach to separating blue multiple quantum wells (MQWs) from sapphire substrates, by selectively removing a heavily doped n-GaN interlayer using electrochemical etching. After fabrication, an ultra-thin FS film exhibits a drastically enhanced photoluminescence (PL) intensity by 17 times normal to the surface. The FS film can be easily lifted-off and transferred to an external substrate by applying a tiny external shear force between the etched and unetched layers. With this method, we finally demonstrate a proof-of-concept transferable LED with clear blue emission under electrical injection.
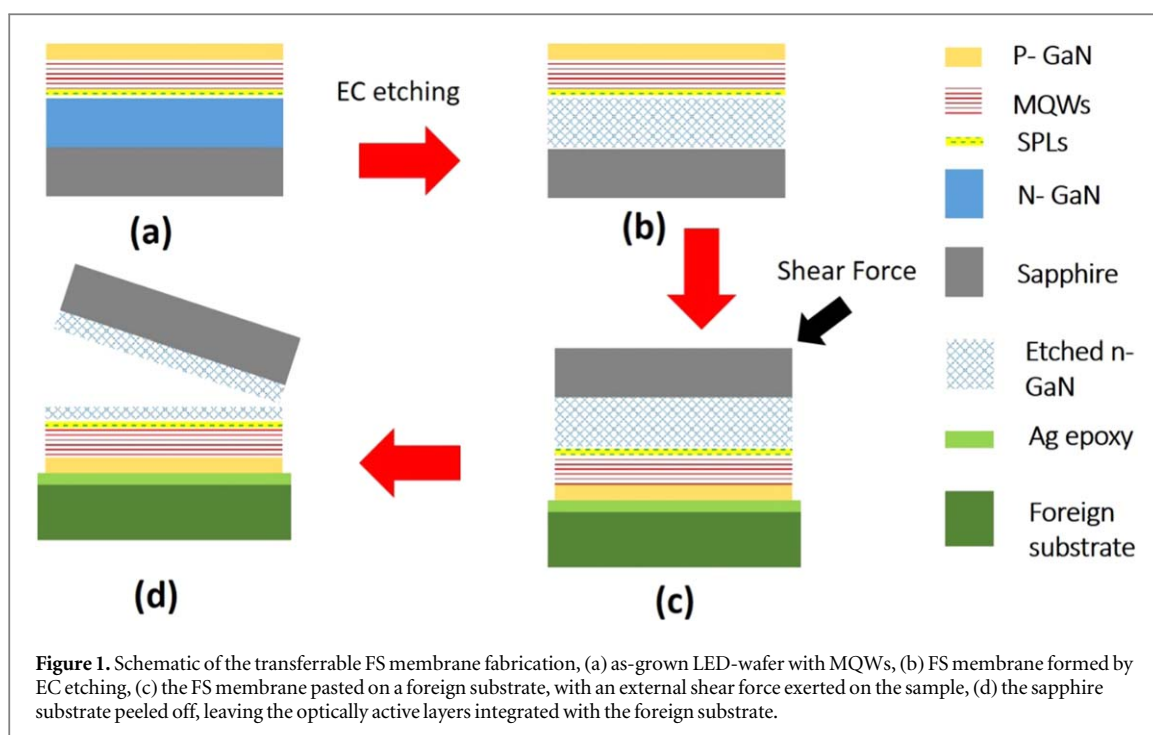
2. Experiments

The sample employed in this work is a commercial blue-LED wafer grown by metal-organic vapour deposition (Xiamen Powerway Advanced Material, Co. Ltd, China). The wafer contains a 220 nm p-GaN layer (with a doping concentration of $\sim6 \times 10^{17}$ cm^{-3}), 10-pair multi-quantum wells (well/barrier thickness = 3/14 nm) above the super-lattices (SPLs), and a 2.5 μm thick n-GaN layer (with a doping concentration of $\sim1 \times 10^{19}$ cm^{-3}), grown on c-plane sapphire substrate. The wafer was diced into 0.5 $\times$ 1 cm^2 stripes to perform the electrochemical etching implemented in 3.5 M HNO$_3$ acid solution, with external bias supplied by a source-meter (Keithley 2400). After etching, the morphology of the samples was inspected by scanning electron microscope (SEM). Steady-state PL was measured using a monochromator (Horiba iR-320, Japan) equipped with a thermoelectric cooled charge-coupled device, a close-loop helium-cooled cryostat down to 10 K, and a 325 nm He-Cd laser (Kimmon Koha, Japan) as the excitation source. Time resolved PL (TRPL) was carried out by focusing a 375 nm diode laser (pulse width = 40 ps) beam down to $\sim$1 um spot on the sample by a 50$\times$ objective lens. Excited signals were measured by a fast-response photodetector with electronic counting unit. The overall time resolution of the system is less than 100 ps. The optical uniformity was investigated by a commercial confocal PL system (Witec alpha 300R) with a 325 nm laser and a 100$\times$ objective lens. Electroluminescence are measured by source-meter (Keithley 2400) and fibre coupled spectrometer (Ocean optics 2000).

3. Results and discussion

The proposed fabrication procedure is schematically shown in figure 1. The key idea is that a heavily doped n-GaN layer underneath the optically active area is electrochemically etched, such that a free-standing (FS) membrane with the blue MQWs will be obtained (figures 1(a) and (b)). Following this, the sample is placed face-down on an adhesive substrate. By applying a minor shear force, the FS membrane will be detached from the sapphire substrate (figure 1(c)). With such a simple lift-off process, the optically active layers can be transferred to a foreign substrate for further device fabrication (figure 1(d)).
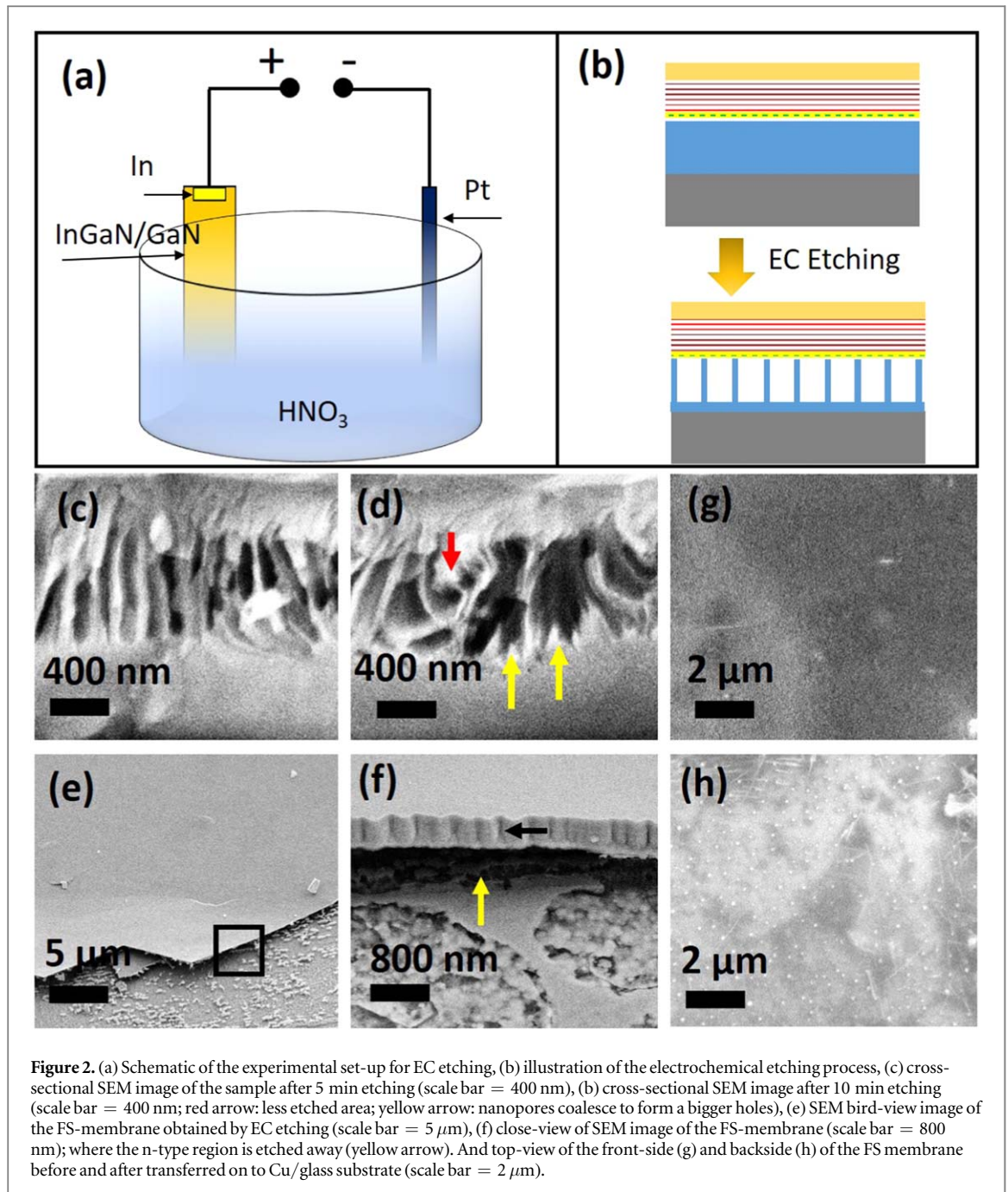
Previous work shows that the morphology of electrochemically etched n-GaN strongly depends on the doping concentration and applied bias [35]. Our experience is similar with previous conclusions. In general, in order to obtain FS membranes, a heavy doping concentration ($>10^{19}$ cm^{-3}) and a large voltage (>10 V) should be used [35]. In addition to this, the etchant concentration is also important. For example, when the HNO$_3$ as the etchant is less than 1 M, nanopores are easily to form; while at a high concentration (>3 M), electro-polishing tends to happen. In our experiment, the electrochemical etching was performed in a 3.5M HNO$_3$ solution with a 15 V bias for 20 min. Figure 2(a) schematically shows the experimental set-up. A piece indium was pasted on a small area where it was pre-etched to n-GaN by inductively coupled plasma (ICP); and a platinum bar was utilized as the counter electrode. Since the electrochemical etching mechanism of GaN has been widely discussed in a number of previous work [35, 36, 44]; here we just briefly explain the etching process. As schematically illustrated in figure 2(b), the electrochemical etching is dominated by oxidation of GaN to generate soluble materials in acidic environment to form a suspending film supported by unetched structures. Initially, nanopores were formed in the n-type GaN layer (figure 2(c)). With increasing etching time, the

Figure 1. Schematic of the transferrable FS membrane fabrication, (a) as-grown LED-wafer with MQWs, (b) FS membrane formed by EC etching, (c) the FS membrane pasted on a foreign substrate, with an external shear force exerted on the sample, (d) the sapphire substrate peeled off, leaving the optically active layers integrated with the foreign substrate.

nanopores intended to grow and to coalescence (yellow arrow in figure 2(d)) to form the suspending membrane, leaving behind some areas less etched (red arrow in figure 2(d)). Figure 2(e) shows the obtained FS membrane, where the bending is due to strain relaxation by electrochemical etching. Figure 2(f) is a close-view of the squared area in figure 2(e)**,** clearly showing hollow regions formed underneath the FS membrane (yellow arrow in figure 2(f)), also named as electropolishing in some literature [45]. In the meantime, we also see that the edges of the thin films are polished during the etching process (black arrow in figure 2(f)). Figure 2(g) exhibits the top view after etching, where a smooth surface is observed. In order to investigate the morphology of the backside, the sample was transferred to a copper coated glass (Cu/Glass) substrate in a facing-down manner, using silver paste as the adhesive material (figure 1(c)). After the silver paste drying out, a slight shear force was exerted to detach the film from sapphire (figure 1). As shown in figure 2(h), unetched n-GaN areas are observed in the backside. The inhomogeneous etching process is likely owing to space charge region formed near defects, which prohibits current flow and thus stops etching. This is under investigation.

The optical properties of our transferred samples are firstly studied by PL measurement at room temperature normal to the sample surface. As shown in figure 3(a), the peak position of the PL spectrum after fabrication locates at 447.5 nm, with a 0.9 nm redshift compared with the as-grown sample (446.6 nm). This observation is in contrary to the blueshift generated from alleviated quantum-confined Stark effect by strain relaxation, as was observed in nanopatterned MQWs. This anti-intuitive phenomenon is worthy of a future investigation, which may be related with the excitation of an ultra-thin film and changing of stain status; leading to band gap narrowing [46–48]. The integrated intensity of the FS membrane is 17-fold higher than that of the as-grown sample, implying a significant improvement of the quantum efficiency. To understand this, we performed temperature-dependent PL (TDPL) measurements from 10 to 300 K. The integrated TDPL intensity as a function of temperature reciprocals is shown in figure 3(b). With increasing temperature, the brightness decreases drastically due to thermally related nonradiative recombination. The data can be well fitted into an Arrhenius relationship with two recombination channels as shown in figure 3(b), i.e., by fitting into

$I(t) = I_0 / \left[1 + A \exp\left(-\frac{E_a}{kT}\right) + B \exp\left(-\frac{E_b}{kT}\right) \right]$ [49, 50], where A and B are fitting parameters, and E_a an E_b are recombination energies with related to the two channels. The fitting parameters A, and B of the as-grown sample (FS membrane) are 15.5 and 0.28 (25.5 and 0.87); and the E_a and E_b of the as-grown (FS membrane) are 0.061 and 0.003 eV (0.243 and 0.007 eV), respectively. Assuming all the thermally activated nonradiative channels, which dominate the nonradiative recombination in our sample, are frozen at 0 K. IQE can be evaluated by using the ratio of room temperature PL intensity over the one at 0 K (I_R/I_0, where I_R and I_0 are PL intensities at room temperature and 0 K.). From our fitting results, we obtained the IQE of the as-grown sample and FS membrane are 37.5% and 41.8%, i.e. an enhancement of 11.5% (with respect to the value of the as-grown sample). The slightly increased IQE is further corroborated by time-resolved PL (TRPL) measurements. As shown in figure 3(c), the decay traces of the as-grown and FS-membrane samples are well fitted into a bi-exponential decay [51]. The carrier life times of the as-grown sample and FS-membrane are 17.0 ns and 18.4 ns, respectively.

Figure 2. (a) Schematic of the experimental set-up for EC etching, (b) illustration of the electrochemical etching process, (c) cross-sectional SEM image of the sample after 5 min etching (scale bar = 400 nm), (b) cross-sectional SEM image after 10 min etching (scale bar = 400 nm; red arrow: less etched area; yellow arrow: nanopores coalesce to form a bigger holes), (e) SEM bird-view image of the FS-membrane obtained by EC etching (scale bar = 5 μm), (f) close-view of SEM image of the FS-membrane (scale bar = 800 nm); where the n-type region is etched away (yellow arrow). And top-view of the front-side (g) and backside (h) of the FS membrane before and after transferred on to Cu/glass substrate (scale bar = 2 μm).

It is known that the radiative recombination dominates the slow part of the carrier life time at room temperature [52, 53]. Therefore, the increased lifetime at room temperature indicates an enhanced IQE.
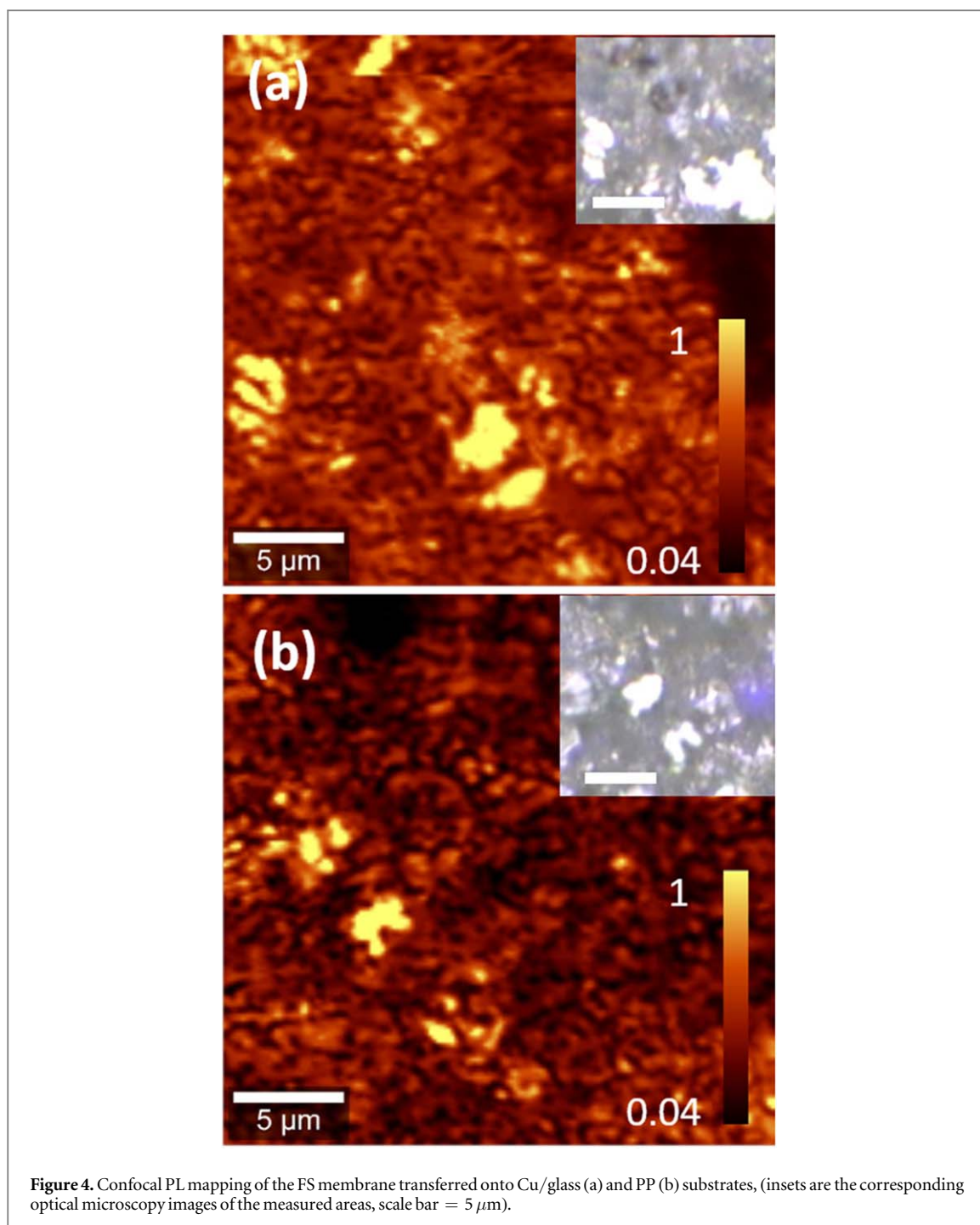
Nevertheless, the enhancement in IQE is much less than 17-fold overall enhancement in the PL intensity, the largest value reported so far. The reflection (14%) from the backside (Ag paste) is also taken into consideration, which also enhances the optical pumping. In the meantime, as the increased surface-to-volume ratio (1.52:1), optical pumping efficiency is further enhanced (we ignored the difference of pumping efficiency between bulk and thin film here). By ruling out all these factors, the total enhancement is still about 8.5 times, attributing to the improved LEE. To verify our hypothesis, we conducted the confocal PL mapping (with a 300 nm spatial resolution, and the objective working distance of 2 mm) to check the optical uniformity. Before this, we fabricate another sample on polypropylene (PP) substrate, with a method identical to the one used on Cu/Glass. Figures 4(a) and (b) show the spatial distribution of PL intensity measured at a centre wavelength of 447 nm with ±20 nm width. It is observed that the position and shape of the 'bright spots' exactly copy those of residual n-GaN clusters (synchronous optical images shown in the inset of figure 4(a) and inset of figure 4(b)). The PL intensity of 'bright spots' is 24 times higher than that in 'flat' region, leading to an average 17 times enhancement on a macro scale. Note that in our experiments, all the PL measurements are measured normal to the sample
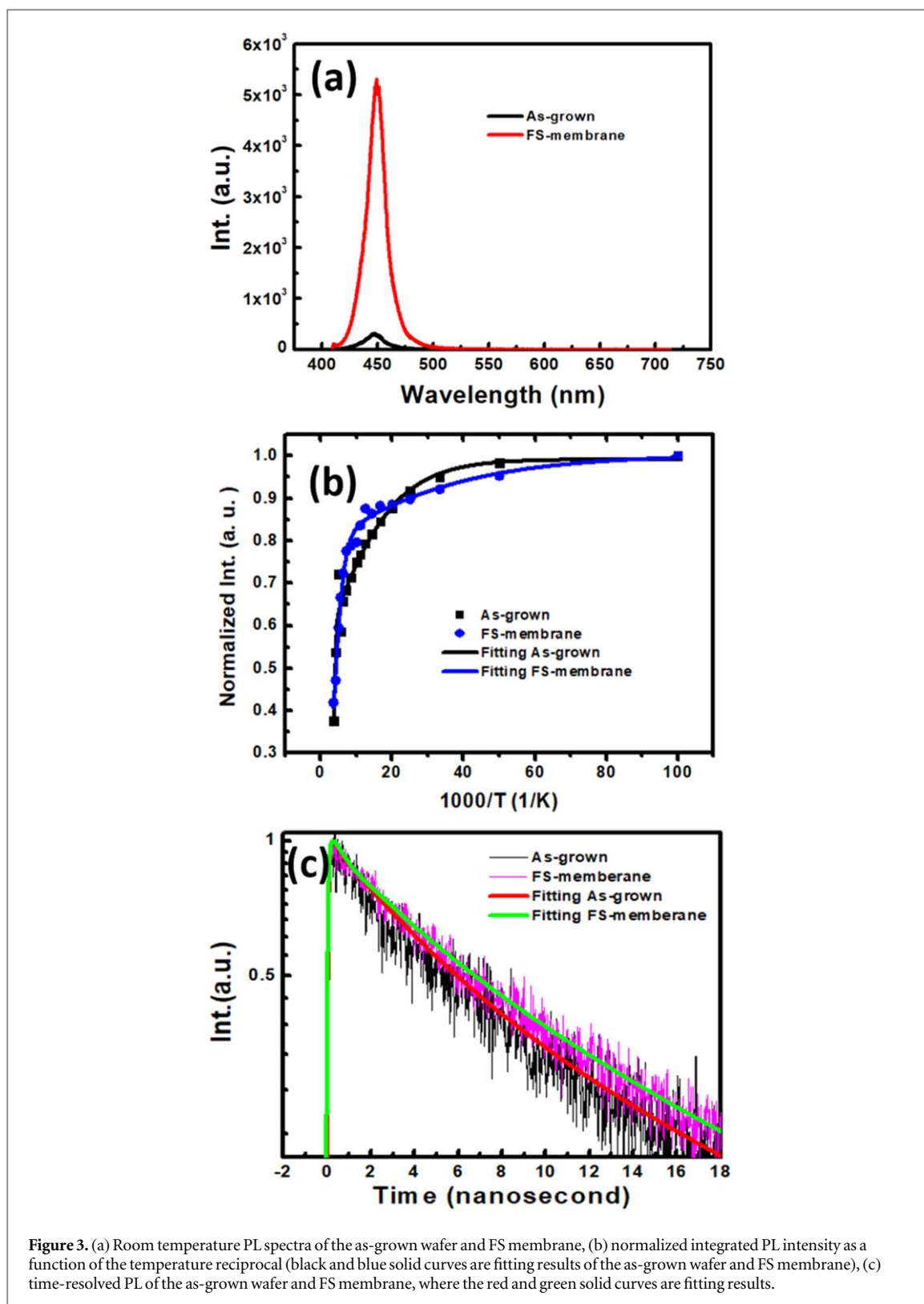
Figure 3. (a) Room temperature PL spectra of the as-grown wafer and FS membrane, (b) normalized integrated PL intensity as a function of the temperature reciprocal (black and blue solid curves are fitting results of the as-grown wafer and FS membrane), (c) time-resolved PL of the as-grown wafer and FS membrane, where the red and green solid curves are fitting results.

surface, which is at the focal plane of collecting lenses. This configuration is subjected to the direction of the emission light, which may lead to errors in the evaluation. Nevertheless, it doesn't affect the decisive conclusion that the enhanced LEE is the dominating role. Detailed research on the mechanism of the enhanced LEE is complicated [54]; and is subjected to further investigations.

To the end of our work, we fabricated proof-of-concept transferrable blue LEDs on Cu/Glass and PP substrates. Silver epoxy is used as the adhesive material (for the transfer) as well as the p-type contact, and Ti(10 nm)/Au(100 nm) rings (200 um the inner diameter and 400 the outer diameter) are deposited by thermal evaporator at room temperature on the residual n-GaN as n-type contact. Inset of figure 5(a) shows the top-view

Figure 4. Confocal PL mapping of the FS membrane transferred onto Cu/glass (a) and PP (b) substrates, (insets are the corresponding optical microscopy images of the measured areas, scale bar = 5 μm).

of the device from an optical microscope (on PP), where small fringes are from the corrugations formed during the transfer. Current-voltage (IV) curves of the devices are shown in figure 5(a). Both devices show similar turn on voltages at 4.7 (on Cu/Glass) and 5.1 V (on PP), higher than the planar devices directly fabricated on an epitaxial wafer (~2.6 V) due to the imperfect ohmic contact in the p-type side [55]. In the meantime, a reverse current of 0.5 mA (corresponding to 1.3 mA cm^{-2}) at -5 V indicates a current leakage (comparing to ~0.1 μA of the planar device fabricated on an epitaxial wafer), possibly due to undesired conducting paths formed during the manual transfer. Electroluminescence (EL) under various injection current are presented in figures 5(b) and (c). By increasing the injection current from 1 to 10 mA, the EL exhibits a bright emission peak at ~437 nm. The integrated intensity of the EL spectra as a function of the injection current is shown in figure 5(d). Both curves exhibit a sublinear behaviour, fitted into $I \propto J^{\alpha}$, where I, J and α are EL intensity, current and fitting parameter, respectively [56]. It is obtained that $\alpha = 0.47$ and 0.3 for the device on Cu/Glass and PP substrates, respectively. The deviation of α from unit value indicates the carriers are not efficiently converted into emitting light. Except for the nonradiative recombination, current leakage and the quality of contacts are supposed to be the major reason. This work demonstrates that electrochemical etching facilitates transferable bule LEDs based on
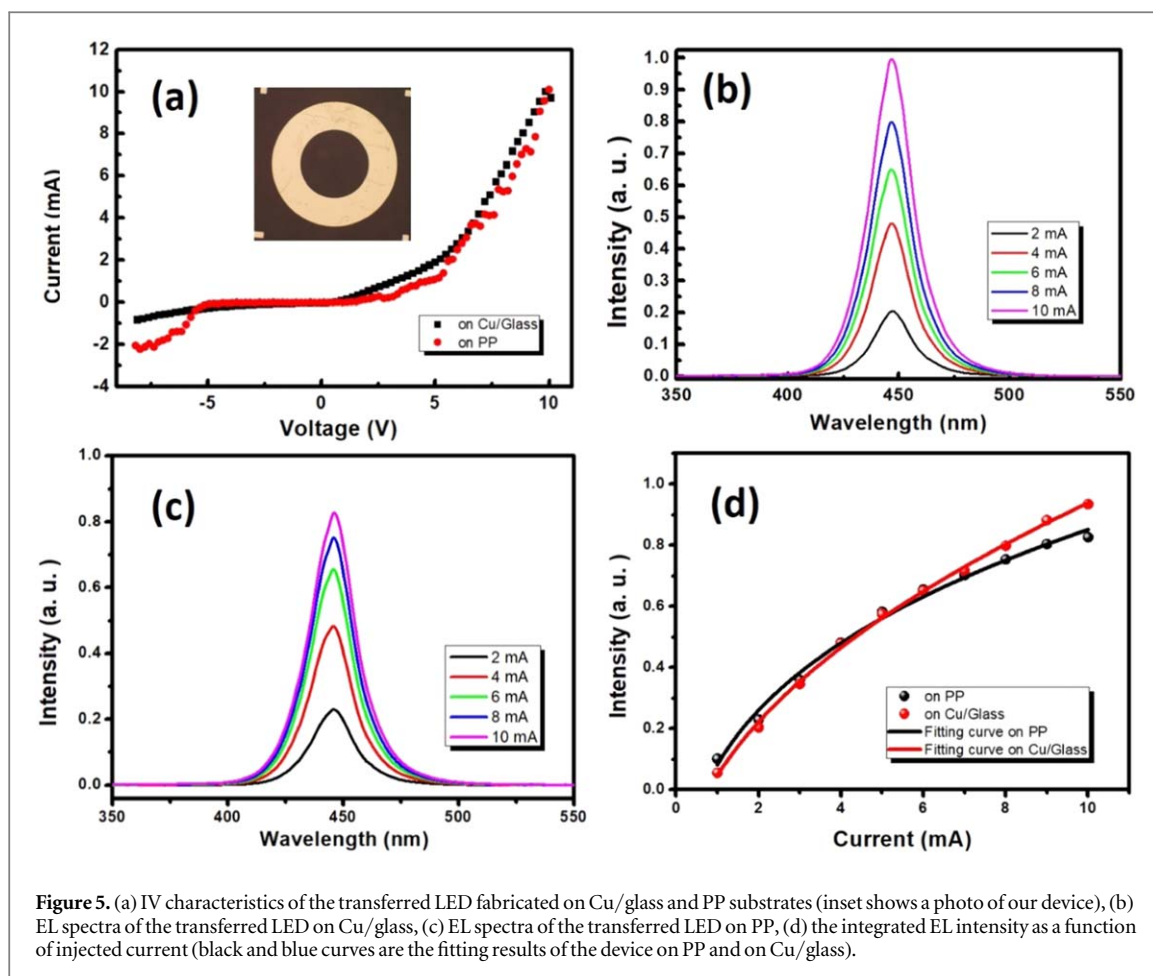
Figure 5. (a) IV characteristics of the transferred LED fabricated on Cu/glass and PP substrates (inset shows a photo of our device), (b) EL spectra of the transferred LED on Cu/glass, (c) EL spectra of the transferred LED on PP, (d) the integrated EL intensity as a function of injected current (black and blue curves are the fitting results of the device on PP and on Cu/glass).

commercial epitaxial wafers. It is worth to point out that the final LED performance depends strongly on the fabrication process, which is a limitation of this work. Nevertheless, there are several ways to further enhance the device performance, (1) One can use double n-type doping layers with one working as the sacrificial layer, which will improve the n-type contact. (2) A better pre-fabricated p-type contact on the device and the foreign substrate. (3) A mechanically controlled transfer process, such as transfer-printing [57].

4. Conclusion

In summary, an ultrathin FS membrane with a thickness of ~420 nm comprising of a full LED structure (p-/n-layers and MQWs) is fabricated using electrochemical etching approach. The membrane can be transferred to arbitrary foreign substrates, such as Cu/Glass or PP, from the host sapphire substrate with a simple lift-off process. The optical properties are massively improved primarily due to the enhanced LEE as a result of surface texturing along with a moderately enhanced IQE. Prototype transferrable blue-LEDs under electrical injection are demonstrated with excellent performance. This work demonstrates a cost-effective technology for transferable blue LEDs without complicated facilities. Therefore, we believe it is important in III-nitride community.

Acknowledgments

ORCID iDs

Yaonan Hou ⓘ https://orcid.org/0000-0001-9618-0701

References

[1] Choi M K, Yang J, Hyeon T and Kim D-H 2018 *Npj Flex. Electron.* **2** 10

[2] Cochrane C, Meunier L, Kell F M and Koncar V 2011 *Indian J. Fibre Text. Res.* **36** 422-428

[3] Lee S Y, Il Park K, Huh C, Koo M, Yoo H G, Kim S, Ah C S, Sung G Y and Lee K J 2012 *Nano Energy* **1** 145

[4] Vega-Colado C *et al* 2018 *Sensors (Switzerland)* **18** 1

[5] Wood V and Bulović V 2010 *Nano Rev.* **1** 5202

[6] Geffroy B, le Roy P and Prat C 2006 *Polym. Int.* **55** 572

[7] Akasaki I 2015 *Ann. Phys.* **527** 311

[8] Nakamura S 2015 *Angew. Chemie - Int. Ed.* **54** 7770

[9] Strite S 1992 *J. Vac. Sci. Technol. B Microelectron. Nanom. Struct.* **10** 1237

[10] Chung K, Lee C-H and Yi G-C 2010 *Science* **330** 655

[11] Yoo H, Chung K, Choi Y S, Kang C S, Oh K H, Kim M and Yi G C 2012 *Adv. Mater.* **24** 515

[12] Chung K, In Park S, Baek H, Chung J-S and Yi G-C 2012 *NPG Asia Mater.* **4** e24

[13] David A, Fujii T, Moran B, Nakamura S, DenBaars S P, Weisbuch C and Benisty H 2006 *Appl. Phys. Lett.* **88** 133514

[14] Chu C F, Lai F I, Chu J T, Yu C C, Lin C F, Kuo H C and Wang S C 2004 *J. Appl. Phys.* **95** 3916

[15] Wong W S, Sands T, Cheung N W, Kneissl M, Bour D P, Mei P, Romano L T and Johnson N M 1999 *Appl. Phys. Lett.* **75** 1360

[16] Damilano B, Lesecq M, Zhou D, Frayssinet E, Chenot S, Brault J, Defrance N, Ebongue A, Cordier Y and Hoel V 2018 *IEEE Photonics Technol. Lett.* **30** 1567

[17] Feng L, Li Y, Xiong H, Wang S, Wang J, Ding W, Zhang Y and Yun F 2016 *Appl. Phys. Express* **9** 081003

[18] Lee H E *et al* 2018 *Adv. Mater.* **30** 1800649

[19] Tian Z *et al* 2018 *Opt. Express* **26** 1817

[20] Krames M R, Shchekin O B, Mueller-Mach R, Mueller G O, Zhou L, Harbers G and Craford M G 2007 *IEEE/OSA J. Disp. Technol.* **3** 160

[21] Kim H-S *et al* 2011 *Proc. Natl Acad. Sci.* **108** 10072

[22] Bae S Y, Kong D J, Lee J Y, Seo D J and Lee D S 2013 *Opt. Express* **21** 535

[23] Strittmatter R P, Beach R A and McGill T C 2001 *Appl. Phys. Lett.* **78** 3226

[24] Park J, Song K M, Jeon S-R, Baek J H and Ryu S-W 2009 *Appl. Phys. Lett.* **94** 221907

[25] Kim D-U, Chang H, Cha H, Jeon H and Jeon S-R 2013 *Appl. Phys. Lett.* **102** 152112

[26] Mishkat-Ul-Masabih S, Luk T S, Rishinaramangalam A, Monavarian M, Nami M and Feezell D 2018 *Appl. Phys. Lett.* **112**

[27] Lin C F, Su C L, Wu H M, Chen Y Y, Huang B S, Huang K L, Shieh B C, Liu H J and Han J 2018 *ACS Appl. Mater. Interfaces* **10** 37725

[28] Kang J H, Jeong D K and Ryu S W 2017 *ACS Appl. Mater. Interfaces* **9** 10637

[29] Chen D and Han J 2012 *Appl. Phys. Lett.* **101** 221104

[30] Zhang Y, Sun Q, Leung B, Simon J, Lee M L and Han J 2011 *Nanotechnology* **22** 045603

[31] Hou Y, Wang Y and Ai Q 2020 *Nanotechnology* **31** 13LT01

[32] Saifaddin B K, Almogbel A S, Zollner C J, Wu F, Bonef B, Iza M, Nakamura S, Denbaars S P and Speck J S 2020 *ACS Photonics* **7** 554

[33] SaifAddin B K, Almogbel A, Zollner C J, Foronda H, Alyamani A, Albadri A, Iza M, Nakamura S, DenBaars S P and Speck J S 2019 *Semicond. Sci. Technol.* **34** 035007

[34] Schwab M J, Han J and Pfefferle L D 2015 *Appl. Phys. Lett.* **106** 241603

[35] Chen D, Xiao H and Han J 2012 *J. Appl. Phys.* **112** 064303

[36] Schwab M J, Chen D, Han J and Pfefferle L D 2013 *J. Phys. Chem. C* **117** 16890

[37] Stonas A R, Margalith T, DenBaars S P, Coldren L A and Hu E L 2001 *Appl. Phys. Lett.* **78** 1945

[38] Hsieh C *et al* 2012 *IEEE Photonics Technol. Lett.* **24** 1775

[39] Hwang D, Yonkee B P, Addin B S, Farrell R M, Nakamura S, Speck J S and DenBaars S 2016 *Opt. Express* **24** 22875

[40] Hsieh C, Su C Y, Weng C M, Chi T T, Kiang Y W and Yang C C 2015 *IEEE Photonics Technol. Lett.* **27** 770

[41] Fujii T, Gao Y, Sharma R, Hu E L, DenBaars S P and Nakamura S 2004 *Appl. Phys. Lett.* **84** 855

[42] Park S H, Zhang C, Yuan G, Chen D and Han J 2015 *ECS Trans.* **66** 143

[43] Kang J H, Ebaid M, Lee J K, Jeong T and Ryu S W 2014 *ACS Appl. Mater. Interfaces* **6** 8683

[44] Park S H, Yuan G, Chen D, Xiong K, Song J, Leung B and Han J 2014 *Nano Lett.* **14** 4293

[45] Muziol G, Siekacz M, Nowakowski-Szkudlarek K, Feduniewicz-Żemuda A, Wony P and Skierbiszewski C 2020 *Nanoscale* **12** 6137

[46] Li H, Chin A H and Sunkara M K 2006 *Adv. Mater.* **18** 216

[47] Li Q, Westlake K R, Crawford M H, Lee S R, Koleske D D, Figiel J J, Cross K C, Fathololoumi S, Mi Z and Wang G T 2011 *Opt. Express* **19** 25528

[48] Dong L, Yadav S K, Ramprasad R and Alpay S P 2010 *Appl. Phys. Lett.* **96** 202106

[49] Chiu C H *et al* 2007 *Nanotechnology* **18** 335706

[50] Lu T *et al* 2015 *Sci. Rep.* **4** 6131

[51] Huang X, Chen R, Zhang C, Chai J, Wang S, Chi D and Chua S J 2016 *Adv. Opt. Mater.* **4** 960

[52] Chichibu S F, Hazu K, Ishikawa Y, Tashiro M, Namita H, Nagao S, Fujito K and Uedono A 2012 *J. Appl. Phys.* **111** 103518

[53] Rosales D, Gil B, Monavarian M, Zhang F, Okur S, Izyumskaya N, Avrutin V, Özgür Ü and Morkoç H 2015 *Pros. SPIE* **9363** 93630J

[54] David A 2013 *IEEE/OSA J. Disp. Technol.* **9** 301

[55] Cho H K *et al* 2006 *Opt. Express* **14** 8654

[56] Hu L, Ren X, Liu J, Tian A, Jiang L, Huang S, Zhou W, Zhang L and Yang H 2020 *Photonics Res.* **8** 279

[57] Rae K *et al* 2018 *Opt. Express* **26** 31474